



Temporal and extratemporal atrophic manifestation of temporal lobe epilepsy using voxel-based morphometry and corticometry: clinical application in lateralization of epileptogenic zone

Majdi Jber¹ · Jafar Mehvari Habibabadi² · Roya Sharifpour^{3,4} · Hengameh Marzbani⁵ · Masoud Hassanpour⁴ · Milad Seyfi^{3,4} · Neda Mohammadi Mobarakeh⁴ · Ahmedreza Keihani³ · Seyed Sohrab Hashemi-Fesharaki⁶ · Mohammadreza Ay^{3,4} · Mohammad-Reza Nazem-Zadeh^{3,4}

Received: 8 August 2020 / Accepted: 14 December 2020
© Fondazione Società Italiana di Neurologia 2021

Abstract

Background Advances in MRI acquisition and data processing have become important for revealing brain structural changes. Previous studies have reported widespread structural brain abnormalities and cortical thinning in patients with temporal lobe epilepsy (TLE), as the most common form of focal epilepsy.

Methods In this research, healthy control cases ($n = 20$) and patients with left TLE ($n = 19$) and right TLE ($n = 14$) were recruited, all underwent 3.0 T MRI with magnetization-prepared rapid gradient echo sequence to acquire T1-weighted images. Morphometric alterations in gray matter were identified using voxel-based morphometry (VBM). Volumetric alterations in subcortical structures and cortical thinning were also determined.

Results Patients with left TLE demonstrated more prevailing and widespread changes in subcortical volumes and cortical thickness than right TLE, mainly in the left hemisphere, compared to the healthy group. Both VBM analysis and subcortical volumetry detected significant hippocampal atrophy in ipsilateral compared to contralateral side in TLE group. In addition to hippocampus, subcortical volumetry found the thalamus and pallidum bilaterally vulnerable to the TLE. Furthermore, the TLE patients underwent cortical thinning beyond the temporal lobe, affecting gray matter cortices in frontal, parietal, and occipital lobes in the majority of patients, more prevalently for left TLE cases. Exploiting volume changes in individual patients in the hippocampus alone led to 63.6% sensitivity and 100% specificity for lateralization of TLE.

✉ Mohammad-Reza Nazem-Zadeh
mnazemzadeh@tums.ac.ir

Majdi Jber
majedy77_@hotmail.com

Jafar Mehvari Habibabadi
dr.mehvari@hotmail.com

Roya Sharifpour
royasharifpour7091@gmail.com

Hengameh Marzbani
marzbani88@gmail.com

Masoud Hassanpour
hasanpour.masoud@gmail.com

Milad Seyfi
milad.seyfi.73@gmail.com

Neda Mohammadi Mobarakeh
nedamohammadi157@gmail.com

Ahmedreza Keihani
AhmadrezaKeihani@gmail.com

Seyed Sohrab Hashemi-Fesharaki
shfesharaki@yahoo.com

Mohammadreza Ay
mohammadreza_Ay@tums.ac.ir

- 1 Medical School, International Campus, Tehran University of Medical Sciences, Tehran, Iran
- 2 Isfahan Neuroscience Research Center, Isfahan University of Medical Sciences, Isfahan, Iran
- 3 Physics and Biomedical Engineering Department, Tehran University of Medical Sciences, Tehran, Iran
- 4 Research Center for Molecular and Cellular Imaging, Advanced Medical Technologies and Equipment Institute (AMTEI), Tehran University of Medical Sciences, Tehran, Iran
- 5 Department of Biomedical Engineering, Amirkabir University of Technology (AUT), Tehran, Iran
- 6 Pars Advanced Medical Research Center, Pars Hospital, Tehran, Iran

Conclusion Alteration of gray matter volumes in subcortical regions and neocortical temporal structures and also cortical gray matter thickness were evidenced as common effects of epileptogenicity, as manifested by the majority of cases in this study.

Keywords Temporal lobe epilepsy · T1-weighted MRI · Voxel-based morphometry · Hippocampus · Volumetric assessment · Lateralization · Cortical thickness · Subcortical structures

Introduction

TLE and establishing the epileptogenic side According to the World Health Organization (WHO), epilepsy is defined as a “chronic neurological disorder affecting the brain at any age from various reasons” distressing at least 50 million people worldwide [1]. Epilepsy has diverse syndromes associated with chronic seizures which differ in frequency contents patient by the patient [2–4]. Temporal lobe epilepsy (TLE) is the most prevalent form of epilepsy in adults. Patients with refractory TLE form the majority of patients referred to epilepsy surgery with at least one-third diagnosed as drug resistant, for whom a resection of unilateral temporal structures such as hippocampus would be a remedy [5, 6]. Intracranial EEG monitoring remains the gold standard for establishing reliably the epileptogenic side [7]. However, it may carry significant risks of infection, hemorrhage, and elevated pressure [8–11]. Therefore, researchers are seeking a reliable way of establishing the side of epileptogenicity by noninvasive neuroimaging markers through biological measurements that may be altered in pathological processes [12]. However, the neuroimaging assessments must be accompanied with computer-aided calculations and quantitative approaches in order to reliably capture the visually nonvisible or barely visible effects of interest from the images.

Hippocampal atrophy as a marker of epileptogenicity About 40% of TLE cases have abnormalities with the shape and positioning of the hippocampus and surrounding structures [13]. High-resolution 3D anatomical T1-weighted imaging by magnetic resonance imaging (MRI) has been used as a technique to evaluate the morphology of the hippocampus and other mesiotemporal lobe structures [14]. Hippocampus volume measurement may serve as a helpful and trusted non-invasive method for clinical lateralizing of TLE [11, 15, 16]. The pattern of atrophy in hippocampus [17] and its subfields [18] could commonly manifest on MRI scans, suggesting an evidence of hippocampal sclerosis as the most common histologic abnormality linked to TLE.

Alterations in other temporal structures There is a common agreement among the scientists that excitotoxic effects of

manifestation of epileptic seizures and deafferentation from the hippocampal efferent fiber loss may consist the mechanisms underlying the initiation and progression of atrophic alterations [19–21].

Group analysis has steadily established that TLE is accompanying with a large degree of brain atrophy extending further into the limbic system and temporal lobe areas, including amygdala and thalamus volumes [22], the anteromedial regions, including the entorhinal cortex, parahippocampal gyrus, and temporal pole [23, 24], and the regions functionally and anatomically connected to the hippocampus [25–27].

Alterations in extratemporal regions Group analysis has shown that the TLE cohorts compared to the healthy control cohorts manifest gray and white matter volume alterations in brain structures beyond the mesial temporal lobe [28, 29], where the degree of atrophy in extrahippocampal regions may be associated with the disease severity [30–32], or the memory deficits [33].

Although it is now a consensus that TLE is associated with significant limbic alteration in individual level [34], the incidence rate for individual extratemporal alterations is not yet established. In other words, it is important to know the chance of extratemporal atrophy for an individual TLE case.

Cortical thickness measurements These measurements can offer a more straight biologically meaningful way for quantifying structural integrity as they respect the folded part of cortical structural anatomy [35]. Different patterns of neocortical atrophy or cortical thinning have been demonstrated by neuroimaging studies [36, 37] supporting findings of morphometric traits [37–39]. Different cortical regions, including the mesiotemporal, limbic, and central sensorimotor cortices, show cerebral cortical thinning in mesial TLE patients in comparison with the control group [38–40]. Cortical thinning appear progressive in patients who have medically intractable epilepsy [39, 41], mostly attributed to the effect of epilepsy such as poor control of seizures [39]. Even though these findings are valid, a relatively similar pattern of cortical thinning is observed in patients who have well-controlled epilepsy seizures [40].

Voxel-based morphometry (VBM) VBM is an automated technique for whole brain analysis to estimate gray matter (GM) concentration surrounding a given voxel. This technique of quantitative MR analysis involves metrics of in vivo assessments for the structural integrity of the human brain [42, 43]. While most of the previous researches have focused on volumetric changes in medial temporal structures, the local morphometric alterations in gray matter and the pattern of cortical thickness change in neocortical temporal, as well as extratemporal regions, are evidenced as important markers for volumetric changes. VBM permits the characterization of regional differences at a local scale having discounted global shape differences [44], bilateral reductions in gray matter volumes [45], and widespread alterations in thalamus volume [46, 47]. It has repeatedly illustrated accurately in lateralizing the seizure focus [14]. It can further demonstrate that brain atrophy extends beyond the visual inspection of MRI images [25, 48].

Problem statement and hypotheses For the clinical standpoint, however, it is vital to determine whether the pattern of subcortical, neocortical, or cortical atrophy is a finding in the majority of TLE patients to be characterized as the expected disease behavior. Comparing the gray matter volume between controls and patients with TLE, we aimed to investigate how frequent the brain atrophy manifests in TLE. We hypothesize that the observed overall atrophy in extrahippocampal and extratemporal structures in TLE cases exhibits as a predominant mechanism and common phenomenon of TLE, implying that the neuronal loss in TLE may incorporate broader regions in temporal and extratemporal areas.

We further hypothesize that multiple computer-aided study of the cortical and subcortical gray matter alterations in TLE patients such as region-based volumetry, voxel-based morphometry, and cortical thickness in stereotaxically defined brain voxels, regions of interest, or surface curvature [26, 48–50] can integrate more reliably into determination of epileptogenic side and patient candidacy for surgical resections.

Methods

Subjects

Patients with refractory TLE were recruited consecutively from those who were referred to the epilepsy long-term monitoring (LTM) clinics. Patients with disabling cognitive impairments or other neurological diseases, presence of other serious systemic or psychological diseases, age more than 55 years old or less than 16 years old, and history of substance or alcohol abuse, pregnancy, and breastfeeding were excluded. For establishing MRI-proven mesial temporal sclerosis, approximated or fully recognizable abnormal alterations in hippocampal imaging attributes including shrinkage in volume and shape on T1-weighted images or hyper signal intensity on T2 FLAIR (fluid attenuated inversion recovery) images were examined.

Along with MRI evidence, to establish the epileptogenic side, diagnostic procedures have been performed based on seizure semiology and video-EEG monitoring compatible with TLE (Table 1):

- (1) Described or observed clinical semiology consistent with seizures of temporal lobe origin: behavioral arrest, staring, right limb dystonia, oral automatism, right versive head/eye deviation, and right limb tonic contraction in left TLE (L-TLE); behavioral arrest, staring, left hand automatism, verbalization, and left versive head/eye deviation in right TLE (R-TLE).
- (2) Electroencephalographic (EEG) evidence of either temporal intermittent rhythmic delta and theta activity or temporal epileptiform discharges identified by the electrode location of spikes and/or slow waves: initial left-sided rhythmic theta and delta activity or spike/spike-wave evolution in L-TLE; initial right-sided rhythmic theta and delta activity or spike/spike-wave evolution in R-TLE.
- (3) Temporal onset seizures captured on EEG indicated by site of onset: left temporal, frontotemporal, or

Table 1 Patient-related clinical and investigative features

Group	Number of cases	Gender (M/F)	Mean age \pm SD	Handedness
HC	20	10/10	27.95 \pm 6.32	19RT/1LT
L-TLE	19	11/8	32.10 \pm 8.47	17RT/1LT/1Both
R-TLE	14	10/4	28.28 \pm 6.28	13RT/1LT
ALL	53	31/22	29.53 \pm 7.29	49RT/3LT/1Both

R right, L left, T temporal, F frontal, P parietal

posterotemporal regions in L-TLE; right temporal, frontotemporal, or posterotemporal regions in R-TLE.

- (4) Interictal irritative zone: left temporal or bilateral with max left temporal in L-TLE; right temporal or bilateral with max right temporal in R-TLE.

Fourteen out of thirty-three patients have undergone surgical resection and have achieved an Engel I outcome after 1 year, confirming the reliability of the applied criteria for establishing the epileptogenic side in cases of TLE. None of the case had undergone phase II intracranial monitoring before the surgery. There were no dual pathologies reported such as tumors, meningitis, or other infections for any of the patients.

All acquired evidence was discussed in a multidisciplinary pre-surgical session, and the consented decision was used as the gold standard for the existence of hippocampal sclerosis as well as an epileptogenic side. This research involved fifty-three subjects, twenty healthy controls, nineteen L-TLE, and fourteen R-TLE subjects. Informed consent was obtained from all participants, had provided approval from the ethical committee at Tehran University of Medical Sciences. Detailed clinical characteristics of patients and control subjects are summarized in Table 2.

Image acquisition

MRI data were collected using a 64-channel phased-array head coil on a 3-Tesla scanner (Siemens Prisma, Erlangen, Germany) with software version “Syngo MR E11” at Iranian National Brain Mapping Laboratory (NMBL). Anatomic images were acquired for clinical diagnosis using a standardized MPRAGE IR protocol for transverse T1-weighted images with the following imaging parameters: TR = 1840 ms, TI = 900 ms, TE = 3.4 ms, flip angle = 8°, matrix = 224 × 224, in-plane resolution = 1.0 × 1.0 mm² slice thickness = 1.0 mm, and pixel bandwidth = 250 Hz/pixel.

Image analysis

Voxel-based morphometry

VBM was conducted using computational anatomical toolbox CAT12 (<http://www.neuro.uni-jena.de/cat>) and statistical parametric map SPM12 (<https://www.fil.ion.ucl.ac.uk/spm/software/spm12>). The Xjview tool was used for visualizing the results (<http://www.alivelearn.net/xjview>). Images were converted to NIFTI format and rigidly reoriented to standard MNI space. The reoriented images were segmented into gray and white matter maps using CAT12 as it obtains a more

sensitive volumetric analysis of the brain regions in comparison with SPM8 [51]. The segmentation employed a mixture model cluster analysis to identify voxel intensities matching particular tissue types (gray matter, white matter, and CSF) combined with an a priori knowledge of the spatial distribution of these tissues in normal subjects, derived from prior probability maps [52]. Modulating in this step, the correction of volumetric changes for segmented images was performed through applying a linear deformation. Subsequently, the signal to noise ratio (SNR) was enhanced through convolution with an isotropic Gaussian kernel of 8×8×8 (denoting the full width half maximum (FWHM) in the X, Y, Z directions), which would further reduce the effect of misregistration between images [53]. For measurement of hippocampus and other ROI subcortical structure volumes, we used Free-Surfer software as a powerful software application suitable for processing and analyzing human brain MRI images (<https://surfer.nmr.mgh.harvard.edu>). It is capable of essential processing steps such as skull stripping, image registration, subcortical segmentation, cortical surface reconstruction, cortical segmentation, and cortical thickness estimation.

Cortical thickness measurement

The essential parts of image processing for evaluating cortical thickness includes skull stripping, inflation of the folded surface tessellation patterns, intensity normalization, segmentation of white matter and gray matter, and ultimately tessellation of the gray/white matter border and automated correction. Then, a deformable surface algorithm is used to obtain the gray/white and gray/cerebrospinal fluid (CSF) surfaces. In this way, both intensity and information from the surfaces in deformation procedures are used to produce representations of cortical thickness. By conducting this, the representations are calculated as the closest distance from the gray/CSF boundary to the gray/white boundary at each vertex on the tessellated surface. Thickness measurements can be mapped on the inflated surface of the brain reconstruction of each subject, allowing visualization of data across the entire cortical surface. Then, the maps determine the areas that show the statistically significant differences between the groups under the study.

Statistical analysis

Voxel-based morphometry

The general linear model (GLM) was used to test our hypothesis [54]. We performed statistical analysis to identify the significant structural changes between the experimental

Table 2 Participants' clinical characteristics

No	Frequency	Onset (years)	Handedness	Semiology (salient features)	Secondary generalization	Ictal EEG	Ictal epileptogenic zone	Interictal irritative zone	Clear MTS evidence on MRI	MRI laterality	Overall laterality	Outcome
1	1-2/w	6	L	Behavioral arrest; right limb dystonia; right facial clonic activity	n	Rhythmic theta activity L > R (T)	L (F < T)	L > R (F < T)	Y	L	L	NA
2	3-4/m	8-9	R	Staring with oral automatisms; right limb dystonia	n	Rhythmic theta activity L > R (F < T)	L (T)	R > L (F < T)	Y	L	L	NA
3	2-3/m	10	R	Bilateral limb automatisms	n	Rhythmic theta activity L = R (T)	L (T)	L = R	N	-	L	NA
4	1-4/m	8	R	Staring with oral automatisms	n	Rhythmic theta activity L > R (T)	L (T)	L > R (F < T)	Y	L	L	NA
5	-	16	R	Bilateral limb automatisms	y	Rhythmic theta activity R (T)	R (T)	R (T)	Y	R	R	NA
6	-	13	R	Bilateral limb automatisms	n	Rhythmic theta activity L (T)	L > R (F < T)	R (T)	Y	R	R	Engel I
7	1-4/m	0.5	R	Behavioral arrest with oral automatisms and blinking	y	Rhythmic theta activity L > R (F < T)	L (T)	R > L (F < T)	N	-	L	NA
8	1-4/m	0.3	R	Behavioral arrest with oral automatisms	n	Rhythmic delta activity L > R (T)	L (T)	L	Y	L	L	NA
9	7-12/w	2	R	Experiential aura; behavioral arrest	n	Rhythmic theta activity L (T)	L (T)	L (T)	Y	L	L	Engel I
10	0.3/m	2	L	Behavioral arrest with staring, oral automatisms, blinking	n	Rhythmic alpha & theta activity R > L (F < T)	R (T)	R = L (T)	Y	R	R	NA
11	1/m	28	R	Behavioral arrest with oral automatisms; verbalization	n	Rhythmic alpha & theta activity R (T)	R (T)	R > L (F < T)	Y	R	R	Engel I
12	7-12/w	0.5	R	Behavioral arrest with staring, left limb automatisms; verbalization; ictal crying	n	Rhythmic theta activity L > R (T > P)	R (T)	R = L (T)	Y	R	R	NA
13	4-7/m	3	R	Left versive motion with left facial and limb y clonic activity; vocalization	y	Rhythmic theta activity R > L (T)	L (T)	R = L (T)	Y	R	R	Engel I
14	4/m	0.6	R	Behavioral arrest with staring; left limb automatisms; verbalization	n	Rhythmic delta activity (T > F), L (T)	R (T)	R (T)	Y	R	R	Engel I
15	0.3-1/m	22	R	Left versive motion; left limb dystonia	n	Rhythmic theta activity L > R (T)	R (T)	R (T)	Y	R	R	Engel I
16	1-4/m	29	R	Behavioral arrest with oral automatisms; left limb automatisms	n	Rhythmic alpha L > R (T > F)	L (T)	L (T)	N	L	L	NA

Table 2 (continued)

No	Frequency	Onset (years)	Handedness	Semiology (salient features)	Secondary generalization	Ictal EEG	Ictal epileptogenic zone	Interictal irritative zone	Clear MTS evidence on MRI	MRI laterality	Overall laterality	Outcome
17	2–3/m	14	R	Behavioral arrest with staring	n	L > R (T)	L (T)	–	Y	L	L	Engel I
18	4/w	3	R	Staring with oral automatisms; right versive y motion, right facial clonic activity	y	Rhythmic theta activity L > R (T)	L (T)	–	Y	L	L	Engel I
19	7–12/m	15	R	Staring with blinking; left versive motion; left limb clonic activity	n	Rhythmic delta activity R > L (T > P), L > R (T)	R > L (T > F)	L = R (T)	N	–	R	NA
20	0.25/m	13	Both	Behavioral arrest with staring	n	–	–	R = L (T)	Y	L	L	NA
21	–	–	R	Behavioral arrest with staring	n	–	L > R (T > F)	–	N	–	L	NA
22	–	–	–	Bilateral limb automatisms	n	–	R (T)	–	Y	R	R	NA
23	1–4/m	11	R	Behavioral arrest with blinking and oral automatisms	n	Rhythmic theta activities L > R (T)	–	L	Y	L	L	Engel I
24	1–4/m	19	R	Behavioral arrest; left limb automatism, right versive motion	n	Rhythmic theta activity L > R (T)	L (T)	L (T)	Y	L	L	Engel I
25	–	–	–	Behavioral arrest with staring	n	–	L (T)	–	N	–	L	Engel I
26	1–12/m	1	R	Behavioral arrest with oral automatisms; left limb automatisms	n	Rhythmic delta activity R > L (T > F) Rhythmic theta activity R (T)	R (T)	R > L (T)	Y	R	R	NA
27	7–12/m	4	L	Experiential aura; behavioral arrest	n	Rhythmic theta activities L > R (T)	L (T)	L (T)	Y	L	L	Engel I
28	1–15/m	2–3	R	Behavioral arrest with blinking; left limb dystonia; ictal laughter	n	Rhythmic alpha activity R > L (T)	R (T)	R (T)	Y	R	R	Engel I
29	1–4/w	17	R	Behavioral arrest; left versive motion; oral automatisms	n	Rhythmic theta activity R (T)	R (T)	(R > L) (T)	Y	R	R	NA
30	3–12/m	7	R	Staring with oral automatisms; right limb dystonia	n	Rhythmic theta activity L > R (T) Bilateral rhythmic delta activity L = R (T)	(L > R) (T)	(L > R) (T > F)	N	–	L	NA
31	2–3/w	2	R	Behavioral arrest with staring and oral automatism, spitting; left limb dystonia	n	Rhythmic theta R > L (T) Rhythmic delta R > L (T > F)	R (T)	R > L (T)	N	R > L	R	Engel I
32	0.3/m	14	R	Bilateral limb automatisms	n	Rhythmic theta activities L > R (T)	L (T)	L (T)	N	–	L	NA
33	0.3/m	18	R	Experiential aura	y	–	L (T)	L (T)	N	–	L	NA

HC healthy control, L-TLE left temporal lobe epilepsy, R-TLE right temporal lobe epilepsy, SD standard deviation, M/F male/female, RT right-handed, LT left-handed

groups. In the basic model of CAT12, we chose analysis of variance (ANOVA) test, since we had three groups of control, L-TLE, and R-TLE. We adjusted the contrast in the final steps of VBM between each group vs. control. Two covariates (total intracranial volume (TIV) and age) have been used in our model. The explicit mask was applied to specify the voxels within the image volume of interest, with the value of absolute threshold masking equaling to 0.2. Multiple-comparison correction was addressed using a false discovery rate (FDR) with a p value set at a 0.05 as the level of significance and K_E -cluster thresholding set to 100. Results were then displayed as overlays on a study-specific template created by normalizing all native space images through transforming followed by measuring the average of warped brain images. To understand whether a temporal or extratemporal morphological process is common mechanism in TLE, we calculate the number of patients undergoing VBM-bases atrophy for the structures with significant mean value between TLE groups and control. Each individual VBM-bases measurement was compared to the corresponding average in control group. Then the incident rate was calculated to decide whether the observed average effect in group analysis is a common phenomenon observed in majority of TLE patients.

Volume measurements of subcortical structures

ANOVA and post hoc Bonferroni for addressing multiple comparisons After extracting volumes of all subcortical segments, we ran ANOVA for three groups using IBM SPSS software version 24. We performed Bonferroni adjustments to address multiple comparisons across brain structures to be able to correlate the significant ROI abnormalities between control, L-TLE, and R-TLE groups. This approach would reveal a subcortical structure(s) that may be useful for lateralizing TLE patients. To understand whether a subcortical morphological process is common mechanism in TLE, we calculate the number of patients undergoing an alteration for the subcortical regions with significant mean value between TLE groups and control. Each individual measurement was compared to the corresponding average in control group. Then the incident rate was calculated to decide whether the observed average effect in group analysis is a common TLE fact.

Hippocampal volumetric for lateralization of TLE Both upper and lower volume thresholds for hippocampus volumetric were established, separating the entire range of these values into three domains, patients with right-side atrophy, patients with left-side atrophy, and other volume measurements not worthy for the lateralization application. The atrophic side would, in turn, be expected to enable prediction of the side

of epileptogenicity. We used control group volume measurements in healthy volunteers as normative data to determine threshold values for decision making on atrophy in TLE cases [15, 55]. The mean normal value minus two standard deviations (SD) defined the lower threshold value, and the mean normal value plus two SD defined the upper threshold value. If a measured value was two SD below or above the mean normal values, they were categorized as right-sided or left-sided atrophy, respectively. On the other hand, if a measured value fell within ± 2 SD of the mean normal values, they were considered non-lateralizing measures.

Cortical thickness measurements

According to Desikan parcellation atlas [56], all cortical thickness regions between control and patient groups were assessed using a vertex-by-vertex general linear model. The mean cortical thickness of each parcellated region was measured and statistically compared using the Query Design Estimate Contrast (QDEC) tool in Free-Surfer. The contrast was assessed between control and patient groups using a two-tailed t test with a p value < 0.05 . Differences were tested using the Student's t tests. The adjusted correction for multiple comparisons was made by considering $0.05/34 = 0.0015$ (where 34 is the number of parcellated regions in each hemisphere of Desikan atlas) as an acceptable upper bound for p value. Thus, we considered each cluster with a p value of < 0.0015 as significant clusters. Finally, cortical thinning clusters location obtained from the GLM with smoothing kernel FWHM equal 20 to show clusters coordinate over the pial surface. To understand whether a cortical morphological process is common mechanism in TLE, we calculate the number of patients undergoing a cortical thinning for the cortical regions with significant mean value between TLE groups and control [37]. Each individual measurement was compared to the corresponding average in control group. Then the incident rate was calculated to decide whether the observed average effect in group analysis is common among TLE cases.

Results

Voxel-based morphometry

In order to get accurate and acceptable VBM results, we first compared spm8 and CAT12 tools. The most important difference between these two toolboxes is their method of segmentation, which can highly affect the results of VBM [42, 57]. Our comparison showed that CAT12 gives more sensitive and

Table 3 Gray matter differences between controls and L-TLE

Comparisons	Region	Hemisphere	<i>t</i> value	MNI coordinates x y z	Cluster size K_E	Incident rate
Structural Shrinkage: L-TLE < control	Temporal lobe	Left	4.4944	-38 14 -38	296	16/19
	Parahippocampal gyrus	Left	5.56	-29 -21 -15	348	16/19
	Hippocampus	Left	5.56	-29 -21 -15	214	18/19
Structural enlargement: L-TLE > control	Frontal lobe	Left	5.17	-38 -11 54	148	15/19
	Cerebrum, occipital lobe	Left	4.70	-8 -89 -11	100	14/19

FDR-corrected results $p < 0.05$

reliable results in a gray matter which is in line with a previous study [51].

Comparison between L-TLE and control

VBM analysis revealed the L-TLE group undergoing significant gray matter volume atrophy compared to the control group (L-TLE < control), with the most significant reductions in left temporal lobe especially in the hippocampus and parahippocampal gyrus, and also in some extratemporal regions of the frontal lobe (Table 3 and Fig. 1, median incident rate of 16 out of 19 cases). We found a reversed effect (structural enlargements; L-TLE > control) for some extratemporal regions in the left cerebrum occipital lobe (Table 3 and Fig. 2, median incident rate of 14 out of 19 cases).

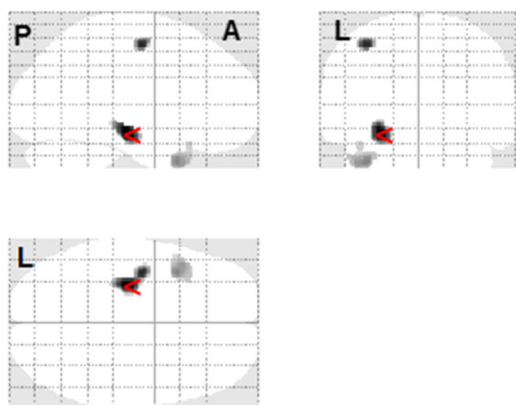


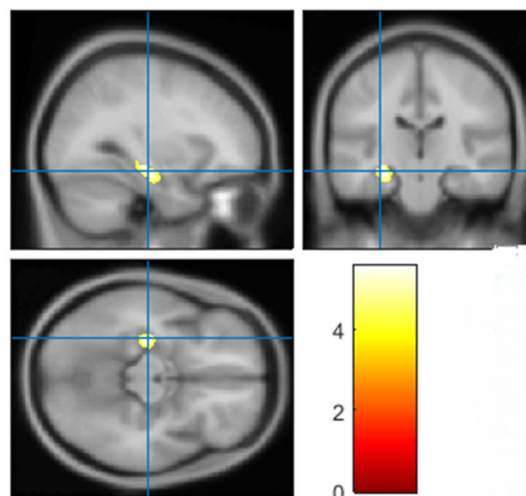
Fig. 1 VBM analysis revealing the L-TLE group undergoing significant volume atrophy in hippocampus and parahippocampal gyrus (temporal lobe) compared to the control group (L-TLE < control). Color scales represent *t*-scores, and the crosshair in each contrast is set to the global

Comparison between R-TLE and control

R-TLE compared to the control group underwent gray matter volume atrophy (R-TLE < control) in the right cerebrum (ipsilateral to the seizure zone), specifically in the right hippocampus (Table 4 and Fig. 3, median incident rate of 10 out of 14 cases). No significant gray matter volume abnormality was observed for the reversed effect.

Comparison between R-TLE and L-TLE

In a direct comparison between R-TLE and L-TLE, we found significant gray matter volume shrinkage in the left temporal lobe especially in the hippocampus and parahippocampal gyrus (L-TLE < R-TLE; Table 5 and Fig. 4). No significant gray



maximum. The gray matter areas with significant volume atrophy were superimposed on the ICBM 152 average template of healthy controls for anatomical reference

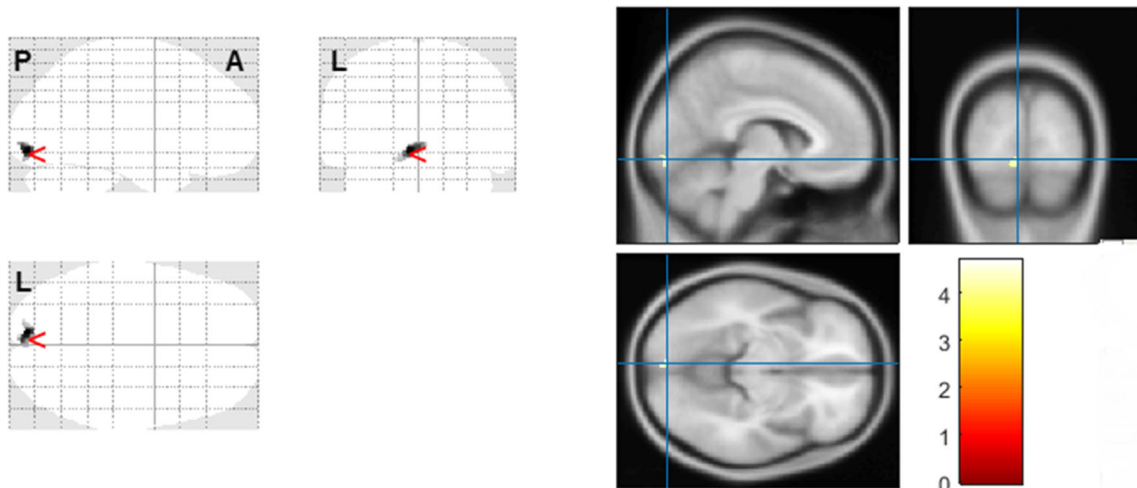


Fig. 2 VBM analysis revealing the L-TLE group undergoing significant volume enlargement in occipital lobe compared to the control group (L-TLE > control). Color scales represent t-scores, and the crosshair in each

contrast is set to the global maximum. The gray matter areas with significant volume enlargement were superimposed on the ICBM 152 average template of healthy controls for anatomical reference

matter volume was observed for the reversed effect (L-TLE > R-TLE).

Alteration of subcortical volumetrics

ANOVA test was carried out on three groups followed by Bonferroni adjustment for multiple comparisons at the 0.05 level of significance on mean volumetric differences between control, L-TLE, and R-TLE groups (Table 6). We found ipsilateral hippocampal volume shrinkage compared to the corresponding side in control for both TLE groups with 95% confidence interval (CI) left hippocampus in L-TLE (p value < 0.0001, incident rate of 19 out of 19 cases) and right hippocampus (p value < 0.001, incident rate of 10 out of 14 cases) in R-TLE groups. However, their contralateral hippocampal volume changes were not statistically significant. Left thalamus proper volume in the L-TLE group was smaller compared to the control group (p value < 0.002, incident rate of 12 out of 19 cases). Pallidum volume in the R-TLE group

underwent bilateral shrinkage compared to the control group (p value < 0.013 and incident rate of 9 out of 14 cases and p value < 0.021 and incident rate of 8 out of 14 cases, for the left and right palladium, respectively). For corpus callosum sub-volumes, we found significant changes for all parts of the L-TLE group in comparison with control group (p values < 0.002, 0.001, 0.0001, and 0.0001, for the posterior, central, mid-anterior, and mid-posterior parts of corpus callosum, respectively, with the median incident rate of 16 out of 19 cases). For R-TLE, only corpus callosum body (mid-anterior and mid-posterior parts) underwent significant atrophy compared to control (p values < 0.029 and 0.004, respectively, with the incident rate of 9 out of 14 cases).

The direct comparison between R-TLE and L-TLE groups (Table 7) revealed that only right and left hippocampi were significant (p values < 0.007 and 0.009 respectively). Therefore, this result was demonstrated appropriate for confidently lateralizing individual TLE patients.

Table 4 Gray matter differences between controls and R-TLE

Comparisons	Region	Hemisphere	t value	MNI coordinates x y z	Cluster size K_E	Incident rate
Structural shrinkage: R-TLE < control	Cerebrum	Right	4.211	26 -32 -5	50	10/14
	Hippocampus	Right	4.211	26 -32 -5	46	10/14

FDR-corrected results p < 0.05 (structural shrinkage: R-TLE < control)

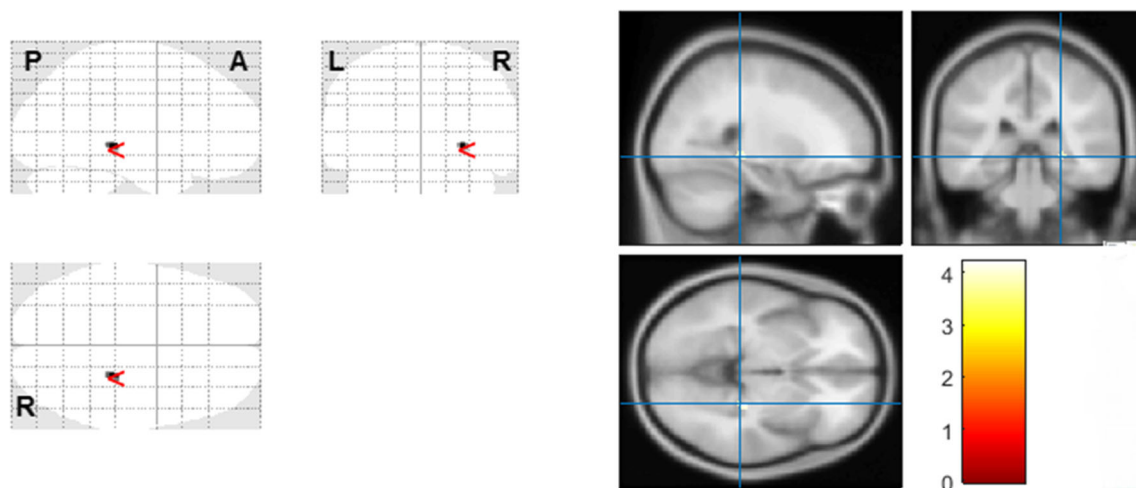


Fig. 3 VBM analysis revealing the R-TLE group undergoing significant gray matter volume atrophy in hippocampus (temporal lobe) compared to the control group (R-TLE < control). Color scales represent t-scores, and

the crosshair in each contrast is set to the global maximum. The gray matter areas with significant volume atrophy were superimposed on the ICBM 152 average template of healthy controls for anatomical reference

For the bilateral subcortical structures with significant differences in volumetrics between control, L-TLE, and R-TLE groups, i.e., thalamus proper, hippocampus, and pallidum (Table 6), we compared the left vs. right sides in control group and ipsilateral vs. contralateral sides in TLE group. Figure 5 shows the standard error plot of these subcortical volumes in mm^3 . Paired t test was performed to compare between the left and right sides of the subcortical structures in control group, which showed no significant difference implying that there was no laterality in subcortical structures for control cases (Fig. 5, top left). Comparison between subcortical volumes of control and TLE groups demonstrated significant bilateral atrophy of thalamus proper, hippocampus, and pallidum for TLE cases compared to control subjects (Fig. 5, top right). Paired t test was also carried out to compare ipsilateral and contralateral sides of the subcortical structures in TLE group, where thalamus proper and hippocampus showed undergoing significant interhemispheric changes (Fig. 5, bottom left). We also compared subcortical volumes of ipsilateral and

contralateral sides of the subcortical structures in TLE group vs. their average values (between left and right) in control group. For TLE cases, the thalamus proper, hippocampus, and pallidum showed significant unilateral atrophy compared to control subjects, including ipsilateral atrophy of all three structures, and contralateral atrophy for thalamus proper and pallidum (Fig. 5, bottom right).

Hippocampal measurements as a biomarker of laterality

The value of normalized “right minus left hippocampal volumes” was used as the laterality index for quantifying unilateral hippocampal atrophy in cases of TLE. Patients with the right (left) epileptogenic side showed a negative (positive) median of -261.6 mm^3 (901.5 mm^3), reflecting right (left)-sided hippocampus atrophy. By this definition of laterality, ten out of fourteen individual R-TLE patients showed a

Table 5 Comparison (L-TLE < R-TLE)

Comparisons	Region	Hemisphere	t value	MNI coordinate x y z	Cluster size KE
Structural alteration: L-TLE < R-TLE	Cerebrum	Left	4.929	-29 -18 -20	246
	Parahippocampal gyrus	Left	4.929	-29 -18 -20	240
	Hippocampus	Left	4.929	-29 -18 -20	133

FDR-corrected results $p < 0.05$

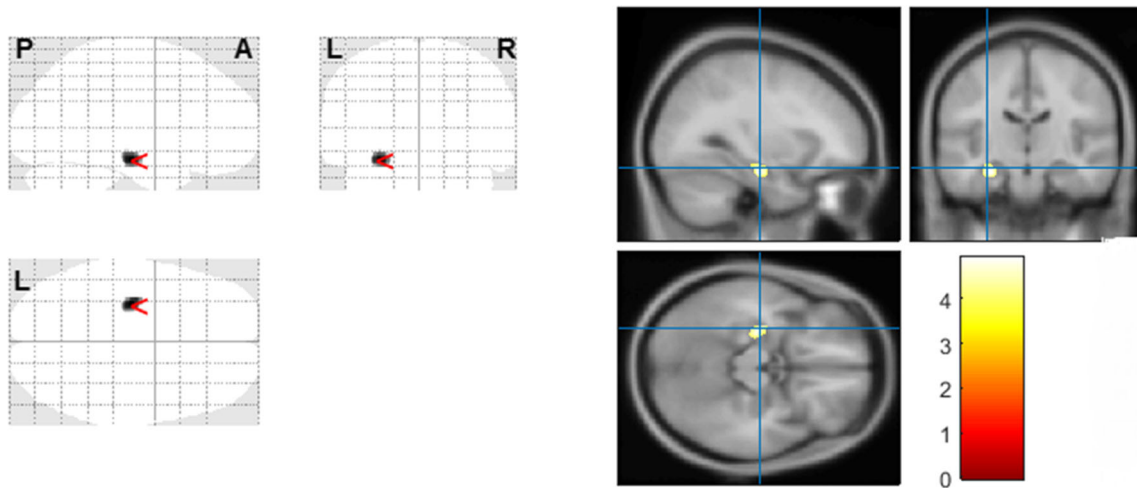


Fig. 4 VBM analysis revealing the L-TLE group undergoing significant gray matter volume atrophy compared to the R-TLE group (L-TLE < R-TLE). Color scales represent t-scores, and the crosshair in each contrast is

set to the global maximum. The gray matter areas with significant volume alteration in these two groups were superimposed on the ICBM 152 average template of healthy controls for anatomical reference

negative laterality index hippocampal volume, while all nineteen individual L-TLE patients had this value greater than zero.

For the second definition with an undecided margin, the upper and lower threshold values (the mean normal value plus/minus two SD) were derived from normative

Table 6 Results of post hoc multiple comparisons, Bonferroni analysis

Temporal structures	Hemisphere	Group (I)	Group (J)	Mean difference in mm ³ (I-J)	Std. deviation	<i>p</i> value**	Incident rate
Hippocampus	Left	Control	L-TLE	819.2*	200.0	0.0001	19/19
		R-TLE		111.5	217.5	1.000	
	Right	Control	L-TLE	150.7	174.7	1.000	10/14
		R-TLE		747.7*	190.07	0.001	
Thalamus proper	Left	Control	L-TLE	1017.5*	285.92	0.002	12/19
		R-TLE		680.0	311.0	0.100	
	Right	Control	L-TLE	498.8	266.6	0.202	
		R-TLE		648.6	290.0	0.089	
Pallidum	Left	Control	L-TLE	232.50	95.3	0.055	
		R-TLE		309.5*	103.7	0.013	
	Right	Control	L-TLE	180.9	86.9	0.128	9/14
		R-TLE		266.7*	94.5	0.021	
Corpus callosum	Posterior	Control	L-TLE	175.6*	49.2	0.002	13/19
		R-TLE		115.6	53.5	0.107	
	Central	Control	L-TLE	169.8*	42.7	0.001	14/19
		R-TLE		114.7	46.5	0.051	
	Mid-anterior	Control	L-TLE	234.3*	48.5	0.0001	17/19
		R-TLE		141.7*	52.8	0.029	
	Mid-posterior	Control	L-TLE	145.0*	31.9	0.0001	16/19
		R-TLE		119.5*	34.7	0.004	

* The mean difference is significant at the 0.05 level of significance. ** *p* values are after Bonferroni adjustment for multiple comparisons

Table 7 ANOVA test with Bonferroni adjustments to compare L-TLE and R-TLE groups

Temporal structures	Hemisphere	Group (I)	Group (J)	Mean difference in mm ³ (I-J)	Std. deviation	p value**	95% confidence interval	
							Lower bound	Upper bound
Hippocampus	Left	R-TLE	L-TLE	707.7*	219.81	0.007	163.0	1252.2
	Right	R-TLE	L-TLE	-597.0*	192.1	0.009	-1072.7	-121.3

*The mean difference is significant at the 0.05 level of Significance. Note that both right and left hippocampus volumes were significantly different between TLE patient groups

data as 541.0 and -297.2 mm³. As can be understood from Table 8, there was no false positive that was detected by this laterality definition for the side of

epileptogenicity based on hippocampal volumetrics, and the proposed method remained completely specific (specificity rate=100%). However, this laterality index

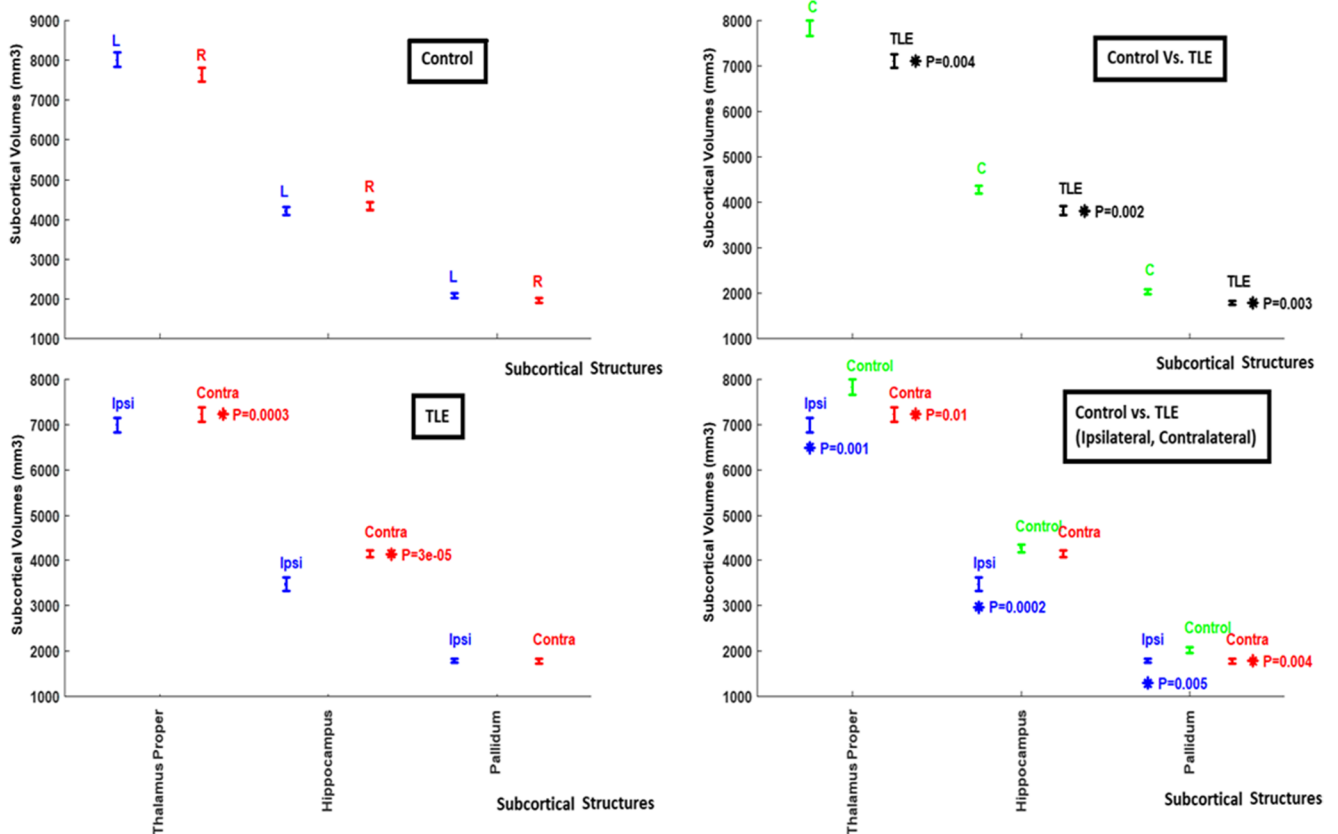


Fig. 5 Standard error plot of the subcortical volumes in mm³ (thalamus proper, hippocampus, and pallidum). Top left: paired comparison between the volumetrics of the left and right sides of the subcortical structures in control group (no significant difference was shown). Top right: comparison between subcortical volumes of control and TLE groups. For TLE cases, the thalamus proper, hippocampus, and pallidum showed significant bilateral atrophy compared to control subjects. Bottom left: paired comparison between ipsilateral and contralateral sides of the subcortical structures in TLE group. Thalamus

proper and hippocampus underwent significant interhemispheric changes. Bottom right: comparison subcortical volumes of ipsilateral and contralateral sides of the subcortical structures in TLE group vs. the average values (between left and right) in control. For TLE cases, the thalamus proper, hippocampus, and pallidum showed significant unilateral atrophy compared to control subjects, including ipsilateral atrophy of all three structures, and contralateral atrophy for thalamus proper and pallidum. Top table note: *Ipsi* ipsilateral, *Contra* contralateral

Table 8 Decision-making on the epileptogenic side in TLE cases based on the hippocampal laterality index

Side of epileptogenicity	Right-side atrophy Hippocampus volume < -297.2 mm ³	Indeterminate (-297.2 < volume < 541.0)	Left-side atrophy hippocampus volume > 541.0 mm ³
Right (<i>n</i> = 14)	8	6	0
Left (<i>n</i> = 19)	0	6	13

based on hippocampal volumetric was not quite sensitive (sensitivity rate = 63.6%), since twelve out of thirty-three TLE cases (six out of fourteen R-TLE and six out of nineteen L-TLE cases) fell within normal occurrence range.

Cortical thickness

Cortical thinning in L-TLE compared to control

The direct comparison of cortical thickness abnormalities between control and L-TLE patient groups revealed clusters of cortical thinning over left hemisphere mainly on parietal and occipital lobes (supramarginal, cuneus), and frontal lobe (caudal middle frontal). Right hemisphere also showed clusters of cortical thinning on frontal lobe (superior frontal, caudal middle frontal), and parietal and occipital lobes (superior parietal). Table 9 illustrates the size of significant clusters, and Fig. 6 shows the clusters over pial surfaces. The median incident rate for the cortical thinning in L-TLE compared to control was 16 out of 19 cases.

Cortical thinning in R-TLE compared to control

The direct comparison of cortical thickness abnormalities revealed a cluster of cortical thinning of R-TLE on the left hemisphere spreading over the frontal lobe (superior frontal), and parietal and occipital lobes (supramarginal). The right hemisphere also showed clusters of cortical thinning with larger sizes over parietal and occipital lobes (supramarginal), and frontal lobe (lateral orbitofrontal). For more details and an illustration of the significant clusters, see Table 10 and Fig. 7. The median incident rate for the cortical thinning in R-TLE compared to control was 10 out of 14 cases.

Unilateral and bilateral cortical thinning

For the bilateral cortical regions with significant differences in cortical thickness between control, L-TLE, and R-TLE groups, i.e., caudal middle frontal, cuneus, superior frontal, and supramarginal gyri, as well as lateral orbitofrontal cortex and superior parietal lobule (Tables 9 and 10), we compared the thickness of the left vs. right cortical regions in control group and ipsilateral vs.

Table 9 Cluster-based *t*-statistic of cortical thinning for control vs. L-TLE

Cluster no	Cluster lobe	Hemisphere	T-statistic	Vertex max	Size (mm ²)	X	Y	Z	Number of vertices	<i>p</i> value	Incident rate
1	Caudal middle frontal (frontal lobe)	Left	3.3228	56,650	2039.52	-38.1	17.9	48.5	3785	0.00047555*	15/19
2	Supramarginal (parietal and occipital)	Left	3.9680	30,376	1109.15	-46.5	-37.0	39.3	2918	0.00010765*	17/19
3	Cuneus (parietal and occipital)	Left	3.0138	12,908	391.45	-17.1	-71.4	15.7	657	0.00096872*	16/19
4	Superior frontal (frontal lobe)	Right	3.9006	72,039	868.58	22.0	27.3	38.9	1600	0.00012572*	16/19
5	Caudal middle frontal (frontal lobe)	Right	3.3821	37,211	418.00	33.6	10.4	32.9	894	0.00041486*	16/19
6	Superior parietal (parietal and occipital lobe)	Right	3.0112	130,216	589.96	16.3	-86.8	37.1	848	0.00097454*	15/19

*The adjusted correction for multiple comparisons were made at *p* value < 0.0015

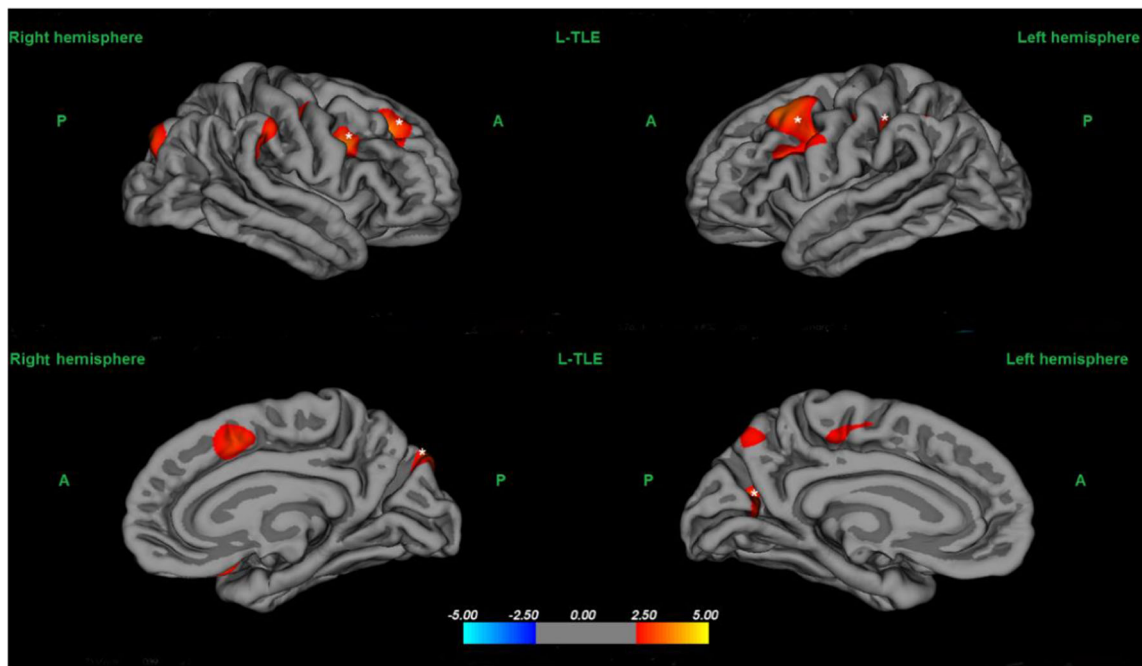


Fig. 6 Cluster-based t-statistic surface maps of cortical thinning in patients with L-TLE vs. control. White stars (*) indicate statistically significant cortical morphometries after adjusted correction for multiple comparisons (p value < 0.0015)

contralateral regions in TLE group. Figure 8 shows the standard error plot of the thickness of these cortical regions in mm . Paired t test was performed to compare between the left and right cortical regions in control group, which showed no significant difference implying that there was no unilateral difference in the thickness of cortical regions for control cases (Fig. 8, top left). Comparison between cortical thickness of control and TLE groups demonstrated significant bilateral cortical thinning in caudal middle frontal, cuneus, and supramarginal gyri, as well as superior parietal lobule for TLE cases compared to control subjects

(Fig. 8, top right). Paired t test was also carried out to compare ipsilateral and contralateral sides of the cortical regions in TLE group, where significant cortical interhemispheric alteration (ipsilateral < contralateral) was seen in caudal middle frontal gyrus (Fig. 8, bottom left). We also compared the thickness of ipsilateral and contralateral regions of the cortical areas in TLE group vs. their average values (between left and right) in control group. For TLE cases, the caudal middle frontal, cuneus, superior frontal, and supramarginal gyri, as well as superior parietal lobule, showed significant contralateral atrophy compared to

Table 10 Cluster-based t-statistic of cortical thinning for control vs. R-TLE

Cluster no	Cluster (lobe)	Hemisphere	T-statistic	Vertex max	Size (mm^2)	X	Y	Z	Number of vertices	p value	Incident rate
1	Superior frontal (frontal lobe)	Left	3.4968	11,260	507.36	-9.0	-11.4	63.3	1235	0.0003185*	11/14
2	Supramarginal (parietal and occipital lobe)	Left	2.9745	150,090	566.41	-46.7	-36.2	37.9	1453	0.0010605*	9/14
3	Lateral orbitofrontal (frontal lobe)	Right	3.0527	160,221	123.07	17.2	13.5	-14.6	304	0.000885*	10/14
4	Supramarginal (Parietal and occipital lobe)	Right	3.5784	74,834	287.85	44.9	-37.4	19.7	725	0.000264*	12/14

*The adjusted correction for multiple comparisons were made at p value < 0.0015

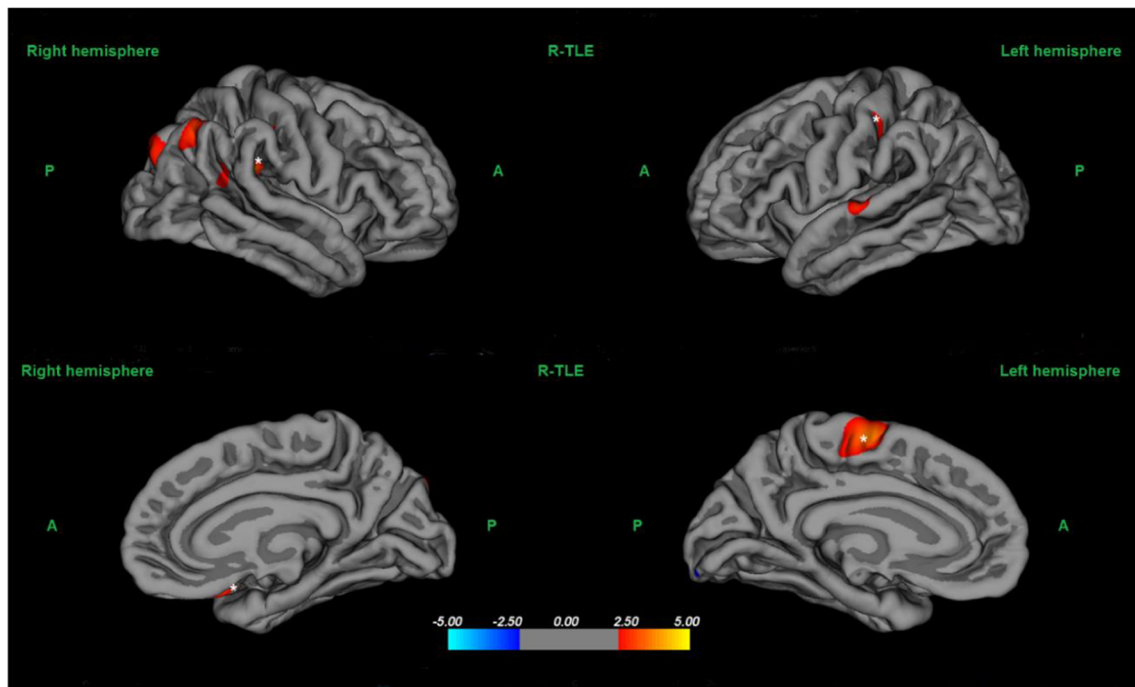


Fig. 7 Cluster-based t-statistic surface maps of cortical thinning in patients with R-TLE vs. control. White stars (*) indicate statistically significant cortical morphometries after adjusted correction for multiple comparisons (p value < 0.0015)

control subjects, along with ipsilateral atrophy in the caudal middle frontal and supramarginal gyri, as well as superior parietal lobule (Fig. 8, bottom right).

Table 11 summarizes all significant findings by different assessment approaches.

Discussion

Neuroimaging techniques are proficient in investigating brain structural changes in patients with epilepsy. Epileptogenicity in the case of TLE may cause hippocampal atrophy [28, 53, 58] as well as cortical thinning in neocortical areas of temporal or extratemporal lobes [59–62].

In our study, VBM analysis detected significant subcortical volumetric atrophy in ipsilateral hippocampus compared to contralateral hippocampus in TLE group as well as bilateral hippocampus in control group. Subcortical volumetry found the thalamus, hippocampus, and pallidum bilaterally vulnerable to the TLE (comparing with control group), with a more pronounced effect in ipsilateral side than contralateral side. Among them, thalamus and hippocampus showed significant atrophy in ipsilateral vs. contralateral side. Cortical thickness analysis showed the cortical regions of bilateral caudal middle

frontal gyrus, cuneus gyrus, and supramarginal gyrus, superior parietal lobule vulnerable to the TLE (comparing to control group), but here with a more pronounced effect in contralateral side than ipsilateral side. Caudal middle frontal gyrus was found to be the only cortical region with significant thinning in ipsilateral side compared to the contralateral side of epileptogenic zone.

There are discrepant findings on the effects of TLE on the volumetric changes in both temporal and extratemporal regions. Some studies demonstrated severe hippocampal atrophy ipsilateral to the epileptogenic [63–68]. Some other studies have reported bilateral hippocampal volume change in right TLE patients [63, 69] and in left TLE [64, 65, 70–74]. In our study, the left TLE showed gray matter loss in left side of the brain mainly in parietal lobe and temporal lobe, especially in parahippocampal gyrus and hippocampus, which is in line with previous studies [26, 28, 53, 58, 75]. For reversed contrast, the left regions in occipital lobe showed statistically significant enlargement in left TLE compared with the control group, however, no enlargement was observed for amygdala despite some other studies [53]. Comparing the right TLE and healthy control group revealed gray matter reduction in the right hemisphere especially in the right hippocampus that is consistent with previous studies [26, 58, 75]. It is worth

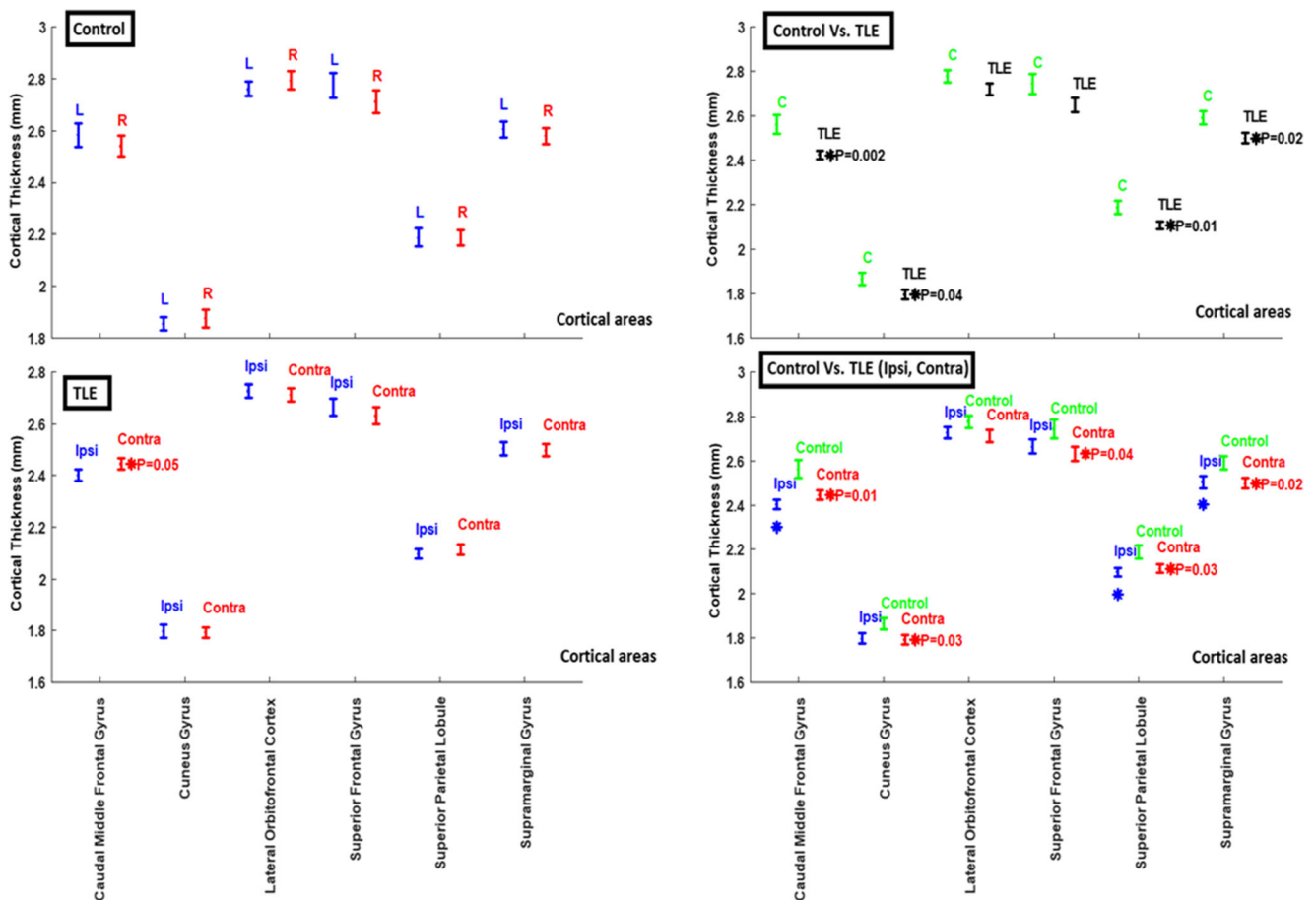


Fig. 8 Standard error plot of the cortical thickness in *mm* (caudal middle frontal, cuneus, superior frontal, and supramarginal gyri, as well as lateral orbitofrontal cortex and superior parietal lobule). Top left: paired comparison between the thickness of the left and right sides of the cortical regions in control group (no significant difference was shown). Top right: comparison between thickness of cortical areas in control and TLE groups. TLE cases showed significant bilateral thinning in caudal middle frontal, cuneus, and supramarginal gyri, as well as superior parietal lobule compared to control subjects. Bottom left: paired comparison between the thickness of ipsilateral and contralateral

cortical regions in TLE group. Cortical interhemispheric alteration (ipsilateral < contralateral) was seen in caudal middle frontal gyrus. Bottom right: comparison between the thickness of ipsilateral and contralateral cortical regions in TLE group vs. the average values (between left and right) in control. For TLE cases, the caudal middle frontal, cuneus, superior frontal, and supramarginal gyri, as well as superior parietal lobule, showed significant contralateral atrophy compared to control subjects, along with ipsilateral atrophy in the caudal middle frontal and supramarginal gyri, as well as superior parietal lobule. Top Table note: *Ipsi* ipsilateral, *Contra* contralateral

mentioning that the size of the regions with significant volume changes in the R-TLE cases was smaller compared to the left TLE cases.

Patients with TLE demonstrate a deviation from typical (left) language lateralization [76]. About 25% of TLE patients show a bilateral or a right-lateralized language function, compared to less than 10% incident rate for healthy subjects (considering right-handed and left-handed together). Atypical language lateralization is most common in left hemispheric epilepsy patients with an acquired injury to the language cortex in childhood. Although less common, but the language functional reorganization has been reported for left hemispheric

epilepsy patients with damage distant to the language cortex or with genetic lesions, as well as for patients with right hemispheric epilepsy. Atypical language lateralization is rare for the left hemispheric epilepsy patients with developmental lesions though [76]. We substantiated in this study that left TLE is more vulnerable than right TLE to the gray matter alterations. The evidenced widespread atrophy in the cortex and subcortical structures in left TLE would be the main cause of atypical language lateralization for TLE patients in general, and our TLE patients in specific, with documented problems in language articulation and comprehension. Nevertheless, we are going to inspect the association of language dominance

Table 11 The summary of findings by different assessments

	Voxel-based morphometry	Subcortical volumetry	Cortical thickness assessment
Left TLE < control	L parahippocampal gyrus, L hippocampus	L hippocampus, L thalamus proper, corpus callosum (posterior, central, mid-anterior, mid-posterior)	L and R caudal middle frontal gyrus, L supramarginal gyrus, L cuneus gyrus, R superior frontal gyrus, R superior parietal gyrus
Right TLE < control	R hippocampus	R hippocampus, R and L pallidum, corpus callosum (mid-anterior, mid-posterior)	L Superior Frontal Gyrus, L & R Supramarginal Gyrus, R Lateral Orbitofrontal Cortex
Left TLE < right TLE	L parahippocampal gyrus, L hippocampus	L hippocampus	–
Right TLE < left TLE	–	R Hippocampus	–
TLE < control	(Bilateral) Hippocampus	(Bilateral) Thalamus, hippocampus, pallidum	(Bilateral) Caudal middle frontal gyrus, cuneus gyrus, supramarginal gyrus, superior parietal lobule
Ipsilateral < control	Hippocampus	Thalamus, hippocampus, pallidum	Caudal middle frontal gyrus, supramarginal gyrus, superior parietal lobule
Contralateral < control	–	Thalamus, pallidum	Caudal middle frontal gyrus, cuneus gyrus, superior frontal gyrus, supramarginal gyrus, superior parietal lobule
Ipsilateral < contralateral	Hippocampus	Thalamus, hippocampus	Caudal middle frontal gyrus

detected by Wada test and neuropsychological evaluations in our TLE patient with the side of epileptogenicity in accordance with exact individual etiology, risk factor, evidence lesions on MRI, onset age and duration of epilepsy, and handedness attributes, and explore the pattern of atypical language lateralization across a variety of our TLE patients.

We found a more severe reduction in gray matter volume of left parahippocampal gyrus and hippocampus in left TLE compared to right TLE cases. In addition to voxel-based morphometry, ROI-based morphometry was performed, where hippocampus was the only subcortical structure that showed a statistically significant difference between the structure volumes of left and right TLE patient groups. Therefore, the hippocampal volume was explored and confirmed as an appropriate candidate for lateralization of TLE.

Prior research has shown that quantitative analysis may identify asymmetry that is not obvious by visual analysis [77]. Quantitative inspections including neuroimaging are

increasingly used as means of lateralizing TLE in attempts to lessen diagnostic ambiguity [16]. Specifically, three-dimensional quantitative inspection on hippocampal volume as an indication of the TLE laterality may be missed by a simple visual inspection, routinely performed two dimensionally. Where a confident lateralization is not possible by presurgical assessments, patients may undergo implantation of intracranial electrodes to clarify the situation and must, in turn, bear the risk of such intervention [16].

In this work, to establish MRI-proven mesial temporal sclerosis (MTS), neuroradiologists visually examined the approximated or fully recognizable abnormal alterations in hippocampal imaging attributes including shrinkage in volume and shape on T1-weighted images, or hyper signal intensity on T2 FLAIR (fluid attenuated inversion recovery) images. Based on all MRI evidence, twenty-three out of thirty-three TLE cases were identified as MTS along with a clear unilateral TLE. Exclusively based on visual inspection of

hippocampal volumes for a large interhemispheric difference and ignoring the hyperintensity of FLAIR signal, only twelve cases were visually identified as MTS. By our quantitative approach, we compared the laterality index (right hippocampus-left hippocampus) to zero, where a negative value indicates right-sided and a positive value suggests a left-side atrophy [15, 55]. This technique lateralized twenty-nine out of thirty-three TLE cases correctly based on hippocampal volume: ten out of fourteen R-TLE patients showed a negative laterality index, and all nineteen L-TLE patients had this value greater than zero. Therefore, four cases showed wrong laterality based on this technique. As a more conservative decision-making, we calculated the mean \pm 2 SD for hippocampal volumes from the control group, by which the laterality index was compared for individual TLE cases [15, 55]. Using this technique, we were able to lateralize the epileptogenic side correctly for twenty-one out of thirty-three patients (63.6% sensitivity) with no false lateralization (100% specificity). Although this technique resulted a lower sensitivity, its specificity is not compromised; thus, it is more reliable and favorable compared to the first technique in real clinical setups. We conclude that this quantitative technique was able to identify nine (27%) more TLE cases than exclusively visual inspections by the neuroradiologists. Nevertheless, we admit that there is evidence of variability in hippocampal volumetrics in unilateral TLE patients [78, 79]. The hippocampal interhemispheric variations can be attributed to subject-specific and genetical factors alone, rather than to actual pathophysiological process of epileptogenicity [10]. Some patients may have significant interhemispheric variations in their hippocampal volumetrics just by natural physiological occurrences, even before they develop epileptogenicity. Furthermore, the epileptogenicity may be expressed interhemispherically variably in each patient [80]. Multiple epilepsy-related confounds including etiologies, seizure etiology, seizure frequency, epilepsy duration, antiepileptic medicine and the used dosage, the number of anticonvulsants, and syndromic presentations may influence the pattern of morphological changes differently across the TLE patients. Therefore, there are active investigations to establish lateralization response models to actually lateralize the site of epileptogenicity based merely upon the pathology-induced interhemispheric variation in the case of a unilateral TLE, beyond the natural physiological occurrences [10, 16]. The direct comparison between control and patient groups revealed that L-TLE has undergone cortical thinning of clusters more than R-TLE mainly in left brain hemisphere. Moreover, the clusters in L-TLE were larger in size in comparison with R-TLE. This is in agreement with the previous research [59–62]. L-TLE demonstrates significant cortical thinning

which has a larger size in left hemisphere in comparison with right hemisphere of the same group. Moreover, R-TLE demonstrates significant cortical thinning mainly in right hemisphere, where the clusters were larger in size in comparison with left hemisphere of the same group. Considering the relatively small sample size, we could not establish a meaningful relation between gray matter abnormalities and other covariates such as seizure frequency. Nevertheless, the VBM may suggest that hippocampal volume atrophy is in correlation with the side of epileptogenicity obtained by electrophysiological and clinical evidence of seizure onset zone. It can be used as evidence of mesial temporal sclerosis for surgical candidacy without undergoing invasive intracranial monitoring.

Conclusion

In this study, we utilized voxel-based morphometry and cortical thickness measurements as quantitative analysis methods to evaluate gray matter abnormalities in temporal lobe epilepsy patients. Our finding evidenced that temporal lobe epilepsy not only alters gray matter structures in subcortical regions but also influences the neocortical temporal structures and cortical gray matter thickness. We found this effect in the majority of the cases, asserting a common effect of epileptogenicity. Our analysis has revealed that left TLE patients are more at risk for cortical thickness abnormalities in comparison with right TLE patients, with more predominant changes for both in the ipsilateral sides in the cortex and subcortical structures. Due to the limited sample size in our study, we were unable to identify the correlation between gray matter atrophy and seizure frequency.

Acknowledgments We must acknowledge the contribution of the Iranian National Brain Mapping Lab (NBNL), and their staffs for MRI data acquisition throughout conducting this project.

Funding This work was partially funded and supported by Iran's National Elites Foundation, National Institute for Medical Research Development (Grant No. 971683), and Cognitive Sciences & Technologies Council (Grant No. 6431), between 2017 and 2019.

Compliance with ethical standards

Conflict of interest The authors declare that they have no conflict of interest.

Ethical approval None

References

- WHO (2019) Epilepsy [WWW Document]. URL <https://www.who.int/news-room/fact-sheets/detail/epilepsy> (accessed 8.21.19)
- Aaberg KM, Surén P, Søråas CL, Bakken IJ, Lossius MI, Stoltenberg C, Chin R (2017) Seizures, syndromes, and etiologies in childhood epilepsy: the International League Against Epilepsy 1981, 1989, and 2017 classifications used in a population-based cohort. *Epilepsia* 58:1880–1891
- Duncan JS, Sander JW, Sisodiya SM, Walker MC (2006) Adult epilepsy. *Lancet* 367:1087–1100
- Hon KL, Leung AKC, Torres AR (2018) Febrile infection-related epilepsy syndrome (fires): an overview of treatment and recent patents. *Recent Patents Inflamm Allergy Drug Discov* 12:128–135
- Chang B, Xu J (2018) Deep brain stimulation for refractory temporal lobe epilepsy: a systematic review and meta-analysis with an emphasis on alleviation of seizure frequency outcome. *Childs Nerv Syst* 34:321–327
- Lee AT, Burke JF, Chunduru P, Molinaro AM, Knowlton R, Chang EF (2019) A historical cohort of temporal lobe surgery for medically refractory epilepsy: a systematic review and meta-analysis to guide future nonrandomized controlled trial studies. *J Neurosurg* 1:1–8
- Blume WT, Holloway GM, Wiebe S (2001) Temporal epileptogenesis: localizing value of scalp and subdural interictal and ictal EEG data. *Epilepsia* 42:508–514
- Arya R, Mangano FT, Horn PS, Holland KD, Rose DF, Glauser TA (2013) Adverse events related to extraoperative invasive EEG monitoring with subdural grid electrodes: a systematic review and meta-analysis. *Epilepsia* 54:828–839
- Meng Y, Voisin MR, Suppiah S, Merali Z, Moghaddamjou A, Alotaibi NM, Manicat-Emo A, Weiss S, Go C, McCoy B (2018) Risk factors for surgical site infection after intracranial electroencephalography monitoring for epilepsy in the pediatric population. *J Neurosurg Pediatr* 22:31–36
- Nazem-Zadeh M-R, Elisevich KV, Schwalb JM, Bagher-Ebadian H, Mahmoudi F, Soltanian-Zadeh H (2014a) Lateralization of temporal lobe epilepsy by multimodal multinomial hippocampal response-driven models. *J Neurol Sci* 347:107–118
- Nazem-Zadeh M-R, Schwalb JM, Bagher-Ebadian H, Mahmoudi F, Hosseini M-P, Jafari-Khouzani K, Elisevich KV, Soltanian-Zadeh H (2014b) Lateralization of temporal lobe epilepsy by imaging-based response-driven multinomial multivariate models, in: 2014 36th Annual International Conference of the IEEE Engineering in Medicine and Biology Society. IEEE, pp. 5595–5598
- Lerch JP, van der Kouwe AJW, Raznahan A, Paus T, Johansen-Berg H, Miller KL, Smith SM, Fischl B, Sotiropoulos SN (2017) Studying neuroanatomy using MRI. *Nat Neurosci* 20:314–326
- Kim H, Chupin M, Colliot O, Bernhardt BC, Bernasconi N, Bernasconi A (2012) Automatic hippocampal segmentation in temporal lobe epilepsy: impact of developmental abnormalities. *Neuroimage* 59:3178–3186
- Duncan JS, Winston GP, Koepp MJ, Ourselin S (2016) Brain imaging in the assessment for epilepsy surgery. *Lancet Neurol* 15:420–433
- Jack R, Cascino D, Zinsmeister AR, Sharbrough W, Hirschorn A, Twomey K (1990) Neuroradiology with MR volume of the hippocampal seizures : measurements 423–429
- Nazem-zadeh M, Schwalb JM, Elisevich KV, Bagher-ebadian H, Hamidian H, Akhondi-asl A, Jafari-khouzani K, Soltanian-zadeh H (2014) Lateralization of temporal lobe epilepsy using a novel uncertainty analysis of MR diffusion in hippocampus, cingulum, and fornix, and hippocampal volume and FLAIR intensity. *J Neurol Sci* 342:152–161. <https://doi.org/10.1016/j.jns.2014.05.019>
- Margerison JH, Corsellis JAN (1966) Epilepsy and the temporal lobes. *Brain* 89:499–530
- Moghaddam HS et al (2020) Distinct patterns of hippocampal subfield volume loss in left and right mesial temporal lobe epilepsy. *Neurol Sci*:1–11
- Berg AT, Berkovic SF, Brodie MJ, Buchhalter J, Cross JH, Van Emde Boas W, Engel J, French J, Glauser TA, Mathern GW, Moshé SL, Nordli D, Plouin P, Scheffer IE (2010) Revised terminology and concepts for organization of seizures and epilepsies: report of the ILAE Commission on Classification and Terminology, 2005-2009. *Epilepsia* 51:676–685. <https://doi.org/10.1111/j.1528-1167.2010.02522.x>
- Mei D, Parrini E, Marini C, Guerrini R (2017) The impact of next-generation sequencing on the diagnosis and treatment of epilepsy in paediatric patients. *Mol Diagn Ther* 21:357–373
- Sutula TP, Hagen J, Pitkänen A (2003) Do epileptic seizures damage the brain? *Curr Opin Neurol* 16:189–195
- Mahmoudi F, Elisevich K, Bagher-Ebadian H, Nazem-Zadeh MR, Davoodi-Bojd E, Schwalb JM, et al(2018). Data mining MR image features of select structures for lateralization of mesial temporal lobe epilepsy. *PLoS One*. 2018;13(8):e0199137
- Alhusaini S, Whelan CD, Doherty CP, Delanty N, Fitzsimons M, Cavalleri GL (2015) Temporal cortex morphology in mesial temporal lobe epilepsy patients and their asymptomatic siblings. *Cereb Cortex* 26:1234–1241
- Bernasconi N, Bernasconi A, Andermann F, Dubeau F, Feindel W, Reutens DC (1999) Entorhinal cortex in temporal lobe epilepsy: a quantitative MRI study. *Neurology* 52:1870–1876
- Bernasconi N, Bernasconi A, Caramanos Z, Antel SB, Andermann F, Arnold DL (2003) Mesial temporal damage in temporal lobe epilepsy: a volumetric MRI study of the hippocampus, amygdala and parahippocampal region. *Brain* 126:462–469
- Bernasconi N, Duchesne S, Janke A, Lerch J, Collins DL, Bernasconi A (2004) Whole-brain voxel-based statistical analysis of gray matter and white matter in temporal lobe epilepsy. *Neuroimage* 23:717–723. <https://doi.org/10.1016/j.neuroimage.2004.06.015>
- Mueller SG, Laxer KD, Barakos J, Cheong I, Garcia P, Weiner MW (2009) Widespread neocortical abnormalities in temporal lobe epilepsy with and without mesial sclerosis. *Neuroimage* 46:353–359
- Alvim MKM, Coan AC, Campos BM, Yasuda CL, Oliveira MC, Morita ME, Cendes F (2016) Progression of gray matter atrophy in seizure-free patients with temporal lobe epilepsy. *Epilepsia* 57:621–629
- Bilevicius E, Yasuda CL, Silva MS, Guerreiro CAM, Lopes-Cendes I, Cendes F (2010) Antiepileptic drug response in temporal lobe epilepsy: a clinical and MRI morphometry study. *Neurology* 75:1695–1701
- Bonilha L, Rorden C, Appenzeller S, Coan AC, Cendes F, Li LM (2006) Gray matter atrophy associated with duration of temporal lobe epilepsy. *Neuroimage* 32:1070–1079
- Coan AC, Appenzeller S, Bonilha L, Li LM, Cendes F (2009) Seizure frequency and lateralization affect progression of atrophy in temporal lobe epilepsy. *Neurology* 73:834–842
- Pittau F, Bisulli F, Mai R, Fares JE, Vignatelli L, Labate A, Naldi I, Avoni P, Parmeggiani A, Santucci M (2009) Prognostic factors in patients with mesial temporal lobe epilepsy. *Epilepsia* 50:41–44

33. Focke NK, Yogarajah M, Bonelli SB, Bartlett PA, Symms MR, Duncan JS (2008) Voxel-based diffusion tensor imaging in patients with mesial temporal lobe epilepsy and hippocampal sclerosis. *Neuroimage* 40:728–737
34. Bonilha L, Elm JJ, Edwards JC, Morgan PS, Hicks C, Lozar C, Rumboldt Z, Roberts DR, Rorden C, Eckert MA (2010) How common is brain atrophy in patients with medial temporal lobe epilepsy? *Epilepsia* 51:1774–1779
35. Lerch J (2007) In-vivo analysis of cortical thickness using magnetic resonance images. *Dissertation Abstracts International: Section B: The Sciences and Engineering* 68(3-B):1467
36. Bonilha L, Keller SS (2015) Quantitative MRI in refractory temporal lobe epilepsy: relationship with surgical outcomes. *Quant Imaging Med Surg* 5:204
37. Whelan CD, Altmann A, Botía JA, Jahanshad N, Hibar DP, Absil J, Alhusaini S, Alvim MKM, Auvinen P, Bartolini E, Berge FPG, Bernardes T, Blackmon K, Braga B, Caligiuri ME, Calvo A, Carr SJ, Chen J, Chen S, Cherubini A, David P, Domin M, Foley S, França W, Haaker G, Isaev D, Keller SS, Kotikalapudi R, Kowalczyk MA, Kuzniecky R, Langner S, Lenge M, Leyden KM, Liu M, Loi RQ, Martin P, Mascalchi M, Morita ME, Pariente JC, Rodríguez-Cruces R, Rummel C, Saavalainen T, Semmler MK, Severino M, Thomas RH, Tondelli M, Tortora D, Vaudano AE, Vivash L, von Podewils F, Wagner J, Weber B, Yao Y, Yasuda CL, Zhang G, Bargalló N, Bender B, Bernasconi N, Bernasconi A, Bernhardt BC, Blümcke I, Carlson C, Cavalleri GL, Cendes F, Concha L, Delanty N, Depondt C, Devinsky O, Doherty CP, Focke NK, Gambardella A, Guerrini R, Hamandi K, Jackson GD, Kälviäinen R, Kochunov P, Kwan P, Labate A, McDonald CR, Meletti S, O'Brien TJ, Ourselin S, Richardson MP, Striano P, Thesen T, Wiest R, Zhang J, Vezzani A, Ryten M, Thompson PM, Sisodiya SM (2018) Structural brain abnormalities in the common epilepsies assessed in a worldwide ENIGMA study. *Brain* 141(2): 391–408
38. Alhusaini S, Doherty CP, Palaniyappan L, Scanlon C, Maguire S, Brennan P, Delanty N, Fitzsimons M, Cavalleri GL (2012) Asymmetric cortical surface area and morphology changes in mesial temporal lobe epilepsy with hippocampal sclerosis. *Epilepsia* 53:995–1003
39. Bernhardt BC, Worsley KJ, Kim H, Evans AC, Bernasconi A, Bernasconi N (2009b) Longitudinal and cross-sectional analysis of atrophy in pharmacoresistant temporal lobe epilepsy. *Neurology* 72:1747–1754
40. Labate A, Cerasa A, Aguglia U, Mumoli L, Quattrone A, Gambardella A (2011) Neocortical thinning in “benign” mesial temporal lobe epilepsy. *Epilepsia* 52:712–717
41. Caciagli L, Bernasconi A, Wiebe S, Koepp MJ, Bernasconi N, Bernhardt BC (2017) A meta-analysis on progressive atrophy in intractable temporal lobe epilepsy: time is brain? *Neurology* 89: 506–516
42. Ashburner J, Friston KJ (2000) Voxel-based morphometry—the methods. *Neuroimage* 11:805–821
43. Mechelli A, Price CJ, Friston KJ, Ashburner J (2005) Voxel-based morphometry of the human brain: methods and applications. *Curr Med Imaging Rev* 1:105–113
44. Godinho R, Domingues V, Crespo EG, Ferrand N (2006) SPM 12 Manual. *Mol Ecol* 15:731–738. <https://doi.org/10.1111/j.1365-294X.2006.02813.x>
45. Boss N, Abela E, Weisstanner C, Schindler K, Wiest R (2019) Local thalamic atrophy associates with large-scale functional connectivity alterations of fronto-parietal cortices in genetic generalized epilepsies. *Clin Transl Neurosci* 3. <https://doi.org/10.1177/2514183x19850325>
46. Bernhardt BC, Rozen DA, Worsley KJ, Evans AC, Bernasconi N, Bernasconi A (2009a) Thalamo–cortical network pathology in idiopathic generalized epilepsy: insights from MRI-based morphometric correlation analysis. *Neuroimage* 46:373–381
47. Huang W, Lu G, Zhang Z, Zhong Y, Wang Z, Yuan C, Jiao Q, Qian Z, Tan Q, Chen G (2011) Gray-matter volume reduction in the thalamus and frontal lobe in epileptic patients with generalized tonic-clonic seizures. *J Neuroradiol* 38:298–303
48. Keller SS, Roberts N (2008) Voxel-based morphometry of temporal lobe epilepsy: an introduction and review of the literature. *Epilepsia* 49:741–757
49. Bonilha L, Rorden C, Castellano G, Pereira F, Rio PA, Cendes F, Li LM (2004) Voxel-based morphometry reveals gray matter network atrophy in refractory medial temporal lobe epilepsy. *Arch Neurol* 61:1379–1384
50. McDonald CR, Ahmadi ME, Hagler DJ, Tecoma ES, Iragui VJ, Gharapetian L, Dale AM, Halgren E (2008) Diffusion tensor imaging correlates of memory and language impairments in temporal lobe epilepsy. *Neurology* 71:1869–1876
51. Farokhian F, Beheshti I, Sone D, Matsuda H (2017) Comparing CAT12 and VBM8 for detecting brain morphological abnormalities in temporal lobe epilepsy. *Front Neurol* 8:428
52. Ashburner J, Friston KJ (2005) Unified segmentation. *Neuroimage* 26:839–851
53. Beheshti I, Sone D, Farokhian F, Maikusa N, Matsuda H (2018) Gray matter and white matter abnormalities in temporal lobe epilepsy patients with and without hippocampal sclerosis. *Front Neurol* 9:107
54. Penny WD, Friston KJ, Ashburner JT, Kiebel SJ, Nichols TE (2006) *Statistical parametric mapping: the analysis of functional brain images. First edition.* University College London, London, UK : Elsevier, 2006
55. Jack CR, Jr., Twomey CK, Zinsmeister AR, Sharbrough FW, Petersen RC, Cascino GD (1989) Anterior temporal lobes and hippocampal formations: normative volumetric measurements from MR images in young adults. *Radiology* 172(2):549–54
56. Desikan RS, Ségonne F, Fischl B, Quinn BT, Dickerson BC, Blacker D, Buckner RL, Dale AM, Maguire RP, Hyman BT, Albert MS, Killiany RJ (2006) An automated labeling system for subdividing the human cerebral cortex on MRI scans into gyral based regions of interest. *Neuroimage* 31:968–980. <https://doi.org/10.1016/j.neuroimage.2006.01.021>
57. Deichmann R, Good CD, Josephs O, Ashburner J, Turner R (2000) Optimization of 3-D MP-RAGE sequences for structural brain imaging. *Neuroimage* 12:112–127
58. Park KM, Kim TH, Mun CW, Shin KJ, Ha SY, Park J, Lee BI, Lee H-J, Kim SE (2018) Reduction of ipsilateral thalamic volume in temporal lobe epilepsy with hippocampal sclerosis. *J Clin Neurosci* 55:76–81
59. Galovic M, Van Dooren VQH, Postma T, Vos SB, Caciagli L, Borzi G, Rosillo JC, Vuong KA, De Tisi J, Nachev P, Duncan JS, Koepp MJ (2019) Progressive cortical thinning in patients with focal epilepsy. *JAMA Neurol* 76:1–10. <https://doi.org/10.1001/jamaneurol.2019.1708>
60. Hong S-J, Bernhardt BC, Schrader DS, Bernasconi N, Bernasconi A (2016) Whole-brain MRI phenotyping in dysplasia-related frontal lobe epilepsy. *Neurology* 86:643–650
61. Kamson DO, Pilli VK, Asano E, Jeong J-W, Sood S, Juhász C, Chugani HT (2016) Cortical thickness asymmetries and surgical outcome in neocortical epilepsy. *J Neurol Sci* 368:97–103

62. Tang Y, An D, Xiao Y, Niu R, Tong X, Liu W, Zhao L, Gong Q, Zhou D (2019) Cortical thinning in epilepsy patients with postictal generalized electroencephalography suppression. *Eur J Neurol* 26: 191–197. <https://doi.org/10.1111/ene.13794>
63. Garcia-Finana M, Denby CE, Keller SS, Wieshmann UC, Roberts N (2006) Degree of hippocampal atrophy is related to side of seizure onset in temporal lobe epilepsy. *Am J Neuroradiol* 27:1046–1052
64. Keller SS, Mackay CE, Barrick TR, Wieshmann UC, Howard MA, Roberts N (2002a) Voxel-based morphometric comparison of hippocampal and extrahippocampal abnormalities in patients with left and right hippocampal atrophy. *Neuroimage* 16:23–31
65. Keller SS, Wieshmann UC, Mackay CE, Denby CE, Webb J, Roberts N (2002b) Voxel based morphometry of grey matter abnormalities in patients with medically intractable temporal lobe epilepsy: effects of side of seizure onset and epilepsy duration. *J Neurol Neurosurg Psychiatry* 73:648–655
66. Mackay CE, Webb JA, Eldridge PR, Chadwick DW, Whitehouse GH, Roberts N (2000) Quantitative magnetic resonance imaging in consecutive patients evaluated for surgical treatment of temporal lobe epilepsy. *Magn Reson Imaging* 18:1187–1199
67. Pitkänen A, Salmenperä T, Kälviäinen R, Partanen K (1998) Hippocampal damage caused by seizures in temporal lobe epilepsy. *Lancet* 351:35
68. Steve TA, Jirsch JD, Gross DW (2014) Quantification of subfield pathology in hippocampal sclerosis: a systematic review and meta-analysis. *Epilepsy Res* 108:1279–1285
69. Pail M, Brázdil M, Mareček R, Mikl M (2010) An optimized voxel-based morphometric study of gray matter changes in patients with left-sided and right-sided mesial temporal lobe epilepsy and hippocampal sclerosis (MTLE/HS). *Epilepsia* 51:511–518
70. Ahmadi ME, Hagler DJ, McDonald CR, Tecoma ES, Iragui VJ, Dale AM, Halgren E (2009) Side matters: diffusion tensor imaging tractography in left and right temporal lobe epilepsy. *Am J Neuroradiol* 30:1740–1747
71. Bonilha L, Rorden C, Halford JJ, Eckert M, Appenzeller S, Cendes F, Li LM (2007) Asymmetrical extra-hippocampal grey matter loss related to hippocampal atrophy in patients with medial temporal lobe epilepsy. *J Neurol Neurosurg Psychiatry* 78:286–294
72. Keller SS, Schoene-Bake J-C, Gerdes JS, Weber B, Deppe M (2012) Concomitant fractional anisotropy and volumetric abnormalities in temporal lobe epilepsy: cross-sectional evidence for progressive neurologic injury. *PLoS One* 7:e46791
73. Kemmotsu N, Girard HM, Bernhardt BC, Bonilha L, Lin JJ, Tecoma ES, Iragui VJ, Hagler DJJ, Halgren E, McDonald CR (2011) MRI analysis in temporal lobe epilepsy: cortical thinning and white matter disruptions are related to side of seizure onset. *Epilepsia* 52:2257–2266. <https://doi.org/10.1111/j.1528-1167.2011.03278.x>
74. Sanjari Moghaddam H, Rahmani F, Aarabi MH, Nazem-Zadeh MR, Davoodi-Bojd E, Soltanian-Zadeh H (2020) White matter microstructural differences between right and left mesial temporal lobe epilepsy. *Acta Neurol Belg* 120(6):1323–31
75. Zheng L, Bin G, Zeng H, Zou D, Gao J, Zhang J, Huang B (2018) Meta-analysis of voxel-based morphometry studies of gray matter abnormalities in patients with mesial temporal lobe epilepsy and unilateral hippocampal sclerosis. *Brain Imaging Behav* 12:1497–1503
76. Briellmann RS, Labate A, Harvey AS, Saling MM, Sveller C, Lillywhite L, Abbott DF, Jackson GD (2006) Is language lateralization in temporal lobe epilepsy patients related to the nature of the epileptogenic lesion? *Epilepsia* 47(5):916–920
77. Kuzniecky RI, Bilir E, Gilliam F, Faught E, Palmer C, Morawetz R, Jackson G (1997) Multimodality MRI in mesial temporal sclerosis: relative sensitivity and specificity. *Neurology* 49:774–778
78. Cook MJ, Fish DR, Shorvon SD, Straughan K, Stevens JM (1992) Hippocampal volumetric and morphometric studies in frontal and temporal lobe epilepsy. *Brain* 115:1001–1015
79. Jack CR Jr, Sharbrough FW, Twomey CK, Cascino GD, Hirschorn KA, Marsh WR, Zinsmeister AR, Scheithauer B (1990) Temporal lobe seizures: lateralization with MR volume measurements of the hippocampal formation. *Radiology* 175:423–429
80. Keihaninejad S, Heckemann RA, Gousias IS, Hajnal JV, Duncan JS, Aljabar P, Rueckert D, Hammers A (2012) Classification and lateralization of temporal lobe epilepsies with and without hippocampal atrophy based on whole-brain automatic MRI segmentation. *PLoS One* 7

Publisher's note Springer Nature remains neutral with regard to jurisdictional claims in published maps and institutional affiliations.